Translocation of a semiflexible polymer through a nanopore in the presence of attractive binding particles

Ramesh Adhikari and Aniket Bhattacharya*
Department of Physics, University of Central Florida, Orlando, Florida 32816-2385, USA
(Received 1 June 2015; published 14 September 2015; corrected 18 March 2016)

We study the translocation dynamics of a semiflexible polymer through a nanopore from the *cis* into the *trans* compartment containing attractive binding particles (BPs) using the Langevin dynamics simulation in two dimensions. The binding particles accelerate the threading process in two ways: (i) reducing the back-sliding of the translocated monomer, and (ii) providing the pulling force toward the translocation direction. We observe that for certain binding strength (ϵ_c) and concentration (ρ) of the BPs, the translocation is faster than the ideal ratcheting condition as elucidated by Simon, Peskin, and Oster [M. Simon, C. S. Peskin, and G. F. Oster, Proc. Natl. Acad. Sci. USA **89**, 3770 (1992)]. The asymmetry produced by the BPs at the *trans*-side leads to similarities of this process to that of a driven translocation with an applied force inside the pore manifested in various physical quantities. Furthermore, we provide an analytic expression for the force experienced by the translocating chain as well as for the scaled mean first passage time (MFPT), for which we observe that for various combinations of N, ϵ, and ρ the scaled MFPT ($\langle\tau\rangle/N^{1.5}\rho^{-0.8}$) collapses onto the same master plot. Based on the analysis of our simulation data, we provide plausible arguments with regard to how the scaling theory of driven translocation can be generalized for such a directed diffusion process by replacing the externally applied force with an effective force.

DOI: 10.1103/PhysRevE.92.032711 PACS number(s): 87.15.ap, 82.35.Lr, 82.35.Pq

I. INTRODUCTION

Transfer of biomolecules through a nanopore is a crucial process in living organisms [1] and is equally important in the application of biotechnology [2]. Translocation of biomolecules from the *cis* to the *trans* compartment often requires a driving force. This driven translocation of biomolecules under the influence of external forces has been studied extensively experimentally and using various theoretical and computational methods [2]. However, it is well known in molecular biology that certain transportation of biomolecules occurs without involvement of molecular motors [3,4]. Examples include translocation of polymers in the presence of binding particles (BPs) (e.g., Chaperones) [4–17] and the translocation of chains due to the asymmetric solvent condition, some of which has been studied recently using coarse-grained (CG) models [18–20].

Simon, Peskin, and Oster (SPO) [6], while searching for a generic but a faster mechanism than diffusion, used the *Brownian ratchet* (BR) mechanism [21] to interpret the translocation of proteins, where the BPs present in the *trans* compartment rectify the pure diffusive motion along the translocation direction. The difference between simple diffusion and directed diffusion can be understood quite easily in the context of one-dimensional (1D) diffusion along a line. In a medium characterized by the monomer friction Γ, the diffusion time of the chain of the order of its own contour length $L = (N-1)\sigma \simeq N\sigma$ (N and σ are the number and size of the monomeric building blocks of the chain, respectively) is given by $\tau_{\rm chain} = L^2/2D_{\rm chain}$, where $D_{\rm chain} = k_BT/(N\Gamma)$ is the diffusion coefficient of the chain, and k_B and T are the Boltzmann constant and temperature, respectively. In the simplified 1D model, SPO introduced equally spaced M binding sites along the chain (so that the separation between successive binding sites is $\delta = L\sigma/M$) with the stipulation that the binding particles attach irreversibly once and for all at these sites as soon as these binding sites are available at the *trans* side immediately after translocation [6]. SPO further assumed that once the particles are bound to the specific sites of the chain, the *trans* segment of the chain cannot go back to the *cis* side. For this directed translocation, it is then easy to see that the efficiency for this directed diffusion rectified by ratchet increases M-fold and

$$\tau_{\rm ratchet} = M\delta^2/2D_{\rm chain} = \tau_{\rm chain}/M. \quad (1)$$

However, there are several assumptions in this derivation by SPO, namely the 1D motion of a rod, the ideal ratchet condition, etc., which in reality are not met. For example, biopolymers are semiflexible and not strictly rods, translocation of a rod through a nanopore in most cases is not a 1D diffusion, the binding and unbinding of particles depend on the interaction strength between the particles and the binding sites, which in turn can depend on the surrounding solvent conditions, and the ready availability of the binding particles, which may be kinetically hindered. However, the simplicity of this idea has resulted in exploring how these factors affect a realistic translocation process [8–18] through a nanopore. Zandi *et al.* [8], using Brownian dynamics (BD) simulations for short 1D rigid rods, found the role of BPs is not only limited to the ratchet mechanism but also provides a pulling force in the direction of translocation, which makes the actual translocation process faster than the ideal BR process. Yu *et al.* [9] have repeated the same argument for longer 1D compressible rods. The effects of size mismatch between BPs and binding sites [10–15], sequence-dependent binding affinity [13–15], and some aspects of chain flexibility have also been studied [17].

*Author to whom all correspondence should be addressed: aniket.bhattacharya@ucf.edu

The asymmetry introduced by the presence of BPs at the *trans* compartment introduces several new features of single-file translocation across the pore. In this study, we consider translocation of a semiflexible chain facilitated by attractive BPs present at the *trans* compartment. We demonstrate the similarity as well as the differences of this process with that of the well-studied problem of driven translocation through a nanopore where the force is present only inside the pore [2]. However, unlike the case of driven translocation of a semiflexible chain [22,23], in addition to the chain flexibility, there are other factors, e.g., the concentration and strength of the attractive binding particles affect the translocation process in a nontrivial way, and much more, the interdependency of the various factors is subtle. Despite these additional complications, we have been able to make a thorough analysis of our simulation results, and we came up with algebraic equations that we believe will promote further theoretical work. Before we go to the subsequent sections, we first show some snapshots produced from the coordinates of the translocating chain and the BPs so as to provide a picture (Fig. 1) of how the ratcheting mechanism is affected by chain flexibility and the concentration of BPs, which are explained in detail in Sec. III. These snapshots also help to appreciate the model introduced in the next section. The organization of the rest of the paper is as follows. In Sec. II we briefly discuss the model and the simulation techniques. The results and their interpretation are presented in Sec. III. In Sec. IV we provide a broader perspective of the problem, and we suggest a generalization of our recently proposed scaling ansatz [24] to include other factors that affect the translocation as studied in this paper.

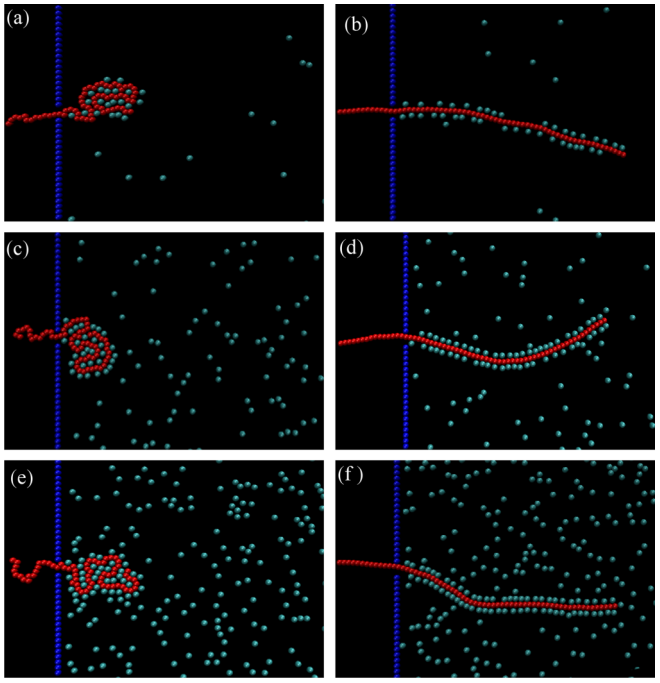

FIG. 1. (Color online) Snapshots of translocation from BD simulations for a fully flexible (left column) and very stiff chain (right column) for three different values of binding particle (BP) densities; (a), (c), and (e) correspond to flexible chains ($\kappa = 0$) and for $\rho =$ 1%, 5%, and 10%, respectively, and (b), (d), and (f) correspond to a stiff chain ($\kappa = 256$) for the same densities. In each case, the lengths of the translocated segments are the same. The cyan circles represent BPs and the red circles depict the chain monomers.

II. MODEL

We have used the bead spring model [25] of a polymer chain with excluded volume, spring, and bending potentials as follows. The excluded volume interaction between any two monomers is given by a short-range Lennard-Jones (LJ) potential,

$$U_{\rm LJ}(r) = 4\epsilon\left[\left(\frac{\sigma}{r}\right)^{12} - \left(\frac{\sigma}{r}\right)^{6}\right] + \epsilon \quad \text{for } r \leqslant 2^{1/6}\sigma$$
$$= 0 \quad \text{for } r > 2^{1/6}\sigma. \tag{2}$$

Here, σ is the effective diameter of a monomer, and ϵ is the strength of the potential. The connectivity between neighboring monomers is modeled as a finite extension nonlinear elastic (FENE) spring with

$$U_{\rm FENE}(r) = -\tfrac{1}{2}kR_0^2 \ln\left(1 - r^2/R_0^2\right), \tag{3}$$

where r is the distance between the consecutive monomers, k is the spring constant, and R_0 is the maximum allowed separation between connected monomers. The chain stiffness is introduced by adding an angle-dependent three-body interaction term between successive bonds as (Fig. 2)

$$U_{\rm bend}(\theta_i) = \kappa_b(1 - \cos\theta_i). \tag{4}$$

Here θ_i is the angle between the bond vectors $\vec{b}_{i-1} = \vec{r}_i - \vec{r}_{i-1}$ and $\vec{b}_i = \vec{r}_{i+1} - \vec{r}_i$, respectively, as shown in Fig. 2. The strength of the interaction is characterized by the bending rigidity κ_b associated with the ith angle θ_i.

The BPs are chosen to be of the same size and mass as that of the polymer beads, and they interact with each other with the same repulsive LJ interaction as given by Eq. (2). The attractive interaction of the BPs with those of the chain monomers is denoted as $U_{\rm binding}$ and is modeled by an attractive LJ interaction with a cutoff distance of 2.5σ and a strength ϵ_c which is kept as a variable parameter in our studies and is given by

$$U_{\rm binding}(r) = 4\epsilon_c\left[\left(\frac{\sigma}{r}\right)^{12} - \left(\frac{\sigma}{r}\right)^{6}\right] + \epsilon \quad \text{for } r \leqslant 2.5\sigma$$
$$= 0 \quad \text{for } r > 2.5\sigma. \tag{5}$$

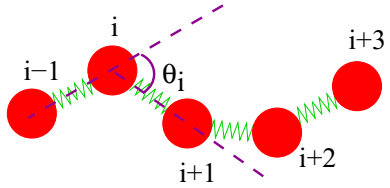

FIG. 2. (Color online) Bead-spring model of a polymer chain with bending angle θ_i subtended by the vectors $\vec{b}_{i-1} = \vec{r}_i - \vec{r}_{i-1}$ and $\vec{b}_i = \vec{r}_{i+1} - \vec{r}_i$.

The strength of the interaction parameter ϵ_c controls the rate of reversible binding and unbinding of the BPs to and from the chain during the translocation process.

The purely repulsive wall consists of one monolayer (line) of immobile LJ particles of diameter σ at $x = 0$. The LJ interaction between the mobile particles (monomers or the BPs) and immobile wall particles is given by

$$U_{\rm W}(r) = 4\epsilon\left[\left(\frac{\sigma}{r}\right)^{12}\right] + \epsilon \quad \text{for } r \leqslant 2^{1/6}\sigma$$
$$= 0 \quad \text{for } r > 2^{1/6}\sigma. \tag{6}$$

The pore is created by removing two particles at the center of the wall. The wall divides a square box into two rectangular compartments on each side (*cis* and *trans*) as shown in Fig. 1. We use the Langevin dynamics with the following equations of motion for the ith monomer,

$$m\ddot{\vec{r}}_i = -\vec{\nabla}(U_{\rm LJ}+U_{\rm FENE}+U_{\rm bend}+U_{\rm W}+U_{\rm binding}) - \Gamma\vec{v}_i + \vec{\eta}_i, \tag{7}$$

and for the ith binding particle as

$$m\ddot{\vec{r}}_i = -\vec{\nabla}(U_{\rm LJ}+U_{\rm W}+U_{\rm binding}) - \Gamma\vec{v}_i + \vec{\eta}_i. \tag{8}$$

Here $\vec{\eta}_i(t)$ is a Gaussian white noise with zero mean at temperature T, and it satisfies the fluctuation-dissipation relation:

$$\langle\vec{\eta}_i(t)\cdot\vec{\eta}_j(t')\rangle = 4k_BT\Gamma\,\delta_{ij}\delta(t-t'). \tag{9}$$

We express length and energy in units of σ and ϵ, respectively. The parameters for the FENE potential in Eq. (3), k and R_0, are set to $k = 500\epsilon/\sigma$ and $R_0 = 1.5\sigma$, respectively. The friction coefficient and the temperature are set to $\Gamma = 0.7\sqrt{m\epsilon/\sigma^2}$ and $k_BT/\epsilon = 1.2$, respectively. The equation of motion is integrated with the reduced unit time step $\Delta t = 0.005$ following the algorithm proposed by van Gunsteren and Berendsen [26].

III. RESULTS

We carried out simulations for chain lengths N from 16 to 256 for different chain rigidity κ_b (in two dimensions, the chain persistence length $\ell_p = 2\kappa_b/k_BT$) and for several choices of concentration ρ and the strength of the attractive interaction ϵ_c for the BPs. Due to a large number of runs for a variety of combinations of parameters, most of our runs are carried out for chain lengths $N = 64$ and 128, respectively, although in certain cases we have extended our calculations for chain length $N = 256$.

The polymer chain is equilibrated for times proportional to $N^{1+2\nu_{2D}}$ (Rouse relaxation time) [27] fixing the first monomer at the pore with the rest of the chain at the *cis* compartment. Here, $\nu_{2D} = 0.75$ is the Flory exponent in two dimensions [27,28]. The chain is then allowed to thread through the pore. When the last monomer exits the pore toward the *trans* compartment, then we stop the simulation and note the translocation time. To get good statistics for all the quantities presented here, we have taken the average over at least 1000 independent runs. We do not apply any external force at the pore to drive the polymer, but the BPs present in the *trans* compartment provide an effective force to make the translocation possible.

In a previous theoretical treatment based on simplified models, polymer translocation has been analyzed in terms of relative time scales of the BPs and the translocating chain [10], i.e., the diffusion time of the BPs ($\tau_{\rm BP}$), the diffusion time for the chain ($\tau_{\rm chain}$), and the MFPT $\langle\tau\rangle$ of the chain, respectively. We define $\tau^1_{\rm chain} \sim \sigma^2/4D_{\rm chain}$ as the diffusion time for the chain to travel a distance of the size of the monomer σ. Likewise, $\tau_{\rm BP} \sim \sigma^2/(4D_{\rm BP})$, where $D_{\rm BP}$ is the diffusion coefficient of the BPs. We have also looked at two other quantities, $\tau_{\rm unocc}$ and $\tau_{\rm occ}$, defined as the average time of the binding sites (chain monomers), which remain unoccupied, and the average time that a BP needs to bind to the chain [10], respectively. For the simpler case of one-dimensional diffusion of a rod, one can show [10] that $\tau_{\rm unocc} \sim \sigma^2/(4\pi\rho D_{\rm BP})$ and $\tau_{\rm occ} \sim \rho\exp(|\beta\epsilon_c|)\tau_{\rm unocc} = \exp(|\beta\epsilon_c|)\sigma^2/D_{\rm BP}$. We have used these estimates to quantify the regimes of our simulation studies in two dimensions.

We have calculated these quantities from the coordinates of the chain and the BPs. In all cases studied here, we find $\tau_{\rm BP} \ll \langle\tau\rangle$ so that the BPs attach almost instantly to the segment of the chain on the *trans* side. Thus the *diffusive regime* characterized by $\tau_{\rm unocc}, \tau_{\rm occ} \gg \tau^1_{\rm chain}$ is absent in our studies. Furthermore, we find that for interaction strength $\epsilon_c/k_BT = 5.0$, $\tau_{\rm occ} \gg \tau_{\rm unocc}, \tau^1_{\rm chain}$, so that for all practical purposes the BPs bind irreversibly during the translocation process, and it is relatively insensitive to the density of the BPs. However, reversible binding and unbinding take place for $\epsilon_c/k_BT = 2.0$, and in this case we find $\tau^1_{\rm chain} \gtrapprox \tau_{\rm occ}, \tau_{\rm unocc}$. We further find that in this case $\tau_{\rm unocc} \geqq \tau_{\rm occ}$ for a low density of the BPs and gets reversed for a larger density of the BPs. This subtle interplay of BP density and interaction strength, as well as the chain flexibility, is a coupled nonlinear problem manifested in several quantities as presented in the next section.

A. Perfect Ratchet and translocation

We begin presenting our results by making a comparison of the MFPT $\langle\tau(s)\rangle$ as a function of the translocation coordinate (s) of the polymer chain in two dimensions for different chain rigidity (κ_b) with the corresponding perfect ratcheting time $\tau_{\rm ratchet}$ shown in Fig. 3 for a chain of length $N = 128$ and binding strength $\epsilon_c = 5\epsilon$ with different concentrations of the BPs ($\rho \simeq 1 - 10\%$) and chain rigidity κ_b ranging from 0 to 256. In each figure, the black dashed line calculated as

$$\tau_{\rm ratchet}(s) = \frac{0.5^2}{2dD_{\rm chain}} + \sum_{i=2}^{i=s}\frac{\delta^2}{2dD_{\rm chain}} \tag{10}$$

represents the perfect ratcheting [9]. Here d is the physical dimension. It is noteworthy in this point that for Brownian dynamics, $D_{\rm chain}$ does not depend on the chain flexibility [29] so that $\tau_{\rm ratchet}$ is the same in Figs. 3(a)–3(c).

Several important conclusions can be drawn from Fig. 3. (i) Translocation is most effective for a fully flexible chain, and beyond a certain density the translocation is faster than the one-dimensional Brownian ratchet (1DBR). (ii) For a given density, the translocation becomes slower for a stiffer chain. (iii) In the limit of a very stiff chain, the translocation time is longer than the 1DBR time except for a high density of BPs.

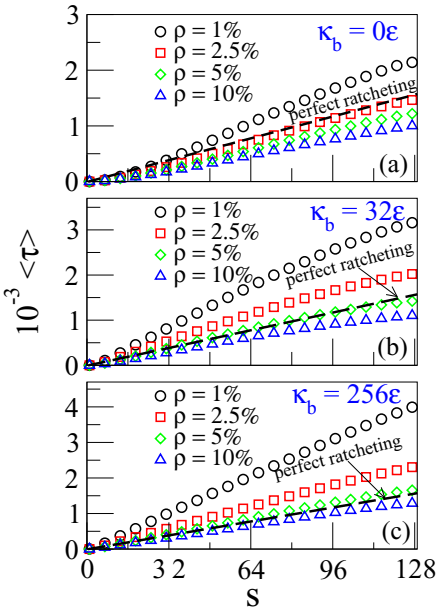

FIG. 3. (Color online) MFPT as a function of the s coordinate for several concentrations of BPs for (a) flexible ($\kappa_b = 0$), (b) semiflexible ($\kappa_b = 32\epsilon$), and (c) stiff ($\kappa_b = 256\epsilon$) polymers. The binding strength is fixed at 5ϵ. The circles (black), squares (red), diamonds (green), and up-triangles (blue) represent the 1%, 2.5%, 5%, and 10% concentration of BPs, respectively, and the black dashed line represents the time for perfect ratcheted motion.

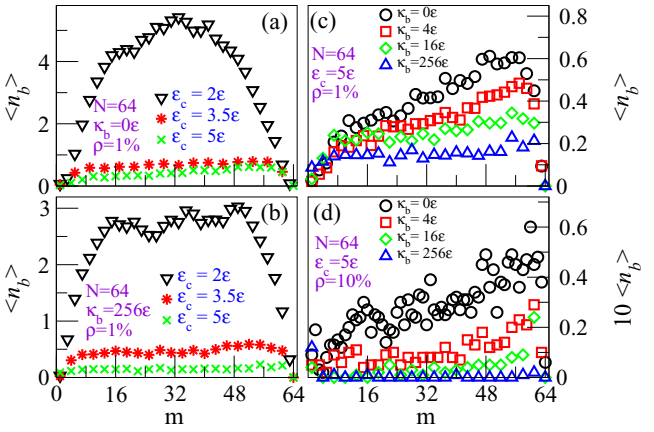

FIG. 4. (Color online) The average number of back-sliding of (a) a *flexible* and (b) a *stiff* chain as a function of monomer index m for different binding strengths when the density of BPs is 1%. In parts (a) and (b), black down-triangles, red stars, and green crosses represent the binding strengths 2ϵ, 3.5ϵ, and 5ϵ, respectively. The same as (a) and (b) but for different chain flexibility (black circles, red squares, green diamonds, and blue up-triangles represent $\kappa_b = 0\epsilon$, 4ϵ, 16ϵ, and 256ϵ, respectively) and fixed binding strength $\epsilon_c = 5\epsilon$ of BPs with density (c) $\rho = 1\%$ and (d) $\rho = 10\%$.

We believe the results are quite general and will be valid for a more realistic situation in three dimensions [30]. Therefore, an efficient design of translocation-based devices may benefit from these conclusions. From our previous studies of driven polymer translocation of semiflexible chains, we know that a stiffer chain translocates slower, which can be explained using the tension propagation (TP) theory of Sakaue [31]. It is tempting to think that the binding particles produce a pulling force and therefore the BP-assisted translocation would share similarities with driven translocation [8]. We will come back to this issue. This result shows that the 1DBR (where the chain cannot slide back) time is not the lower limit for translocation of a semiflexible chain driven by BPs through a nanopore. For a 1D rod, Zandi *et al.* [8] and Yu *et al.* [9] have seen this trend. Our studies establish a far more general result in this context.

B. How efficient is the actual ratcheting mechanism?

The ratcheting of the chain through the pore due to the presence of BPs depends on the density ρ and interaction strength ϵ_c of the binding particles. The chain-flexibility parameter κ_b also plays a crucial role in attractive sites to be available to the binding particles (see Fig. 1). Unlike 1DBR (where once a monomer translocates to the *trans* side it cannot go back to the *cis* side), we expect that there will be some backward translocation for the monomers. Thus in order to study the efficiency of the ratcheting process, we calculate the average of the quantity $n_b(m)$, which represents the number of times the mth monomer goes back and forth from the *cis* to the *trans* side and *vice versa*, before finally exiting to the *trans* side. This captures the back and forth motion of the monomers across the pore. Figure 4(a) shows $\langle n_b(m)\rangle$ as a function of the monomer index m for various combinations of ρ, ϵ_c, and κ_b. A common feature of these plots is that for a low density and a low binding energy, the translocation of the chain is most affected by its flexibility. It is worth noting that when the frequency f_b of binding and unbinding is small, i.e., the time period $T_b = 1/f_b > \langle\tau\rangle$, for all practical purposes we can think that the particles are bound reversibly and make further analysis based on this assumption. However, one can expect qualitative changes in the limit of $T_b = 1/f_b \simeq \langle\tau\rangle$. If the particles bind and unbind several times during the time the chain translocates, this will be reflected in an oscillatory behavior in $\langle n_b\rangle$. Figures 4(a) and 4(b) show $\langle n_b\rangle$ for a fully flexible and very stiff chain for several binding energies. For a fully flexible chain and for weak binding strength $\epsilon_c = 2\epsilon$, $\langle n_b(m)\rangle$ shows a nearly symmetric behavior as a function of the index m, while for a very stiff chain one can clearly see an oscillatory pattern for back-sliding. Figure 1 can help us to have a better physical understanding. For a fully flexible chain, the *trans* segment forms a near-spherical "blob," and beyond a critical size this blob hinders the back-translocation of the incoming monomers; as a result, for a fully flexible chain this back and forth motion saturates and then eventually decreases. On the contrary, for a stiff chain when $\kappa_b \gg \epsilon_c$, the *trans* segment of the chain is relatively straight, and binding and unbinding is relatively insensitive to the monomer index m. However, binding (unbinding) of BPs makes the chain more (less) sluggish, reducing (increasing) the backsliding, which is reflected in the slightly oscillatory behavior. We think for $\epsilon_c \simeq k_BT$ that this will be a generic feature, but it will be hard to see in a simulation, as lowering the strength of the attractive interaction drastically reduces the probability of successful translocation. For $\epsilon_c > k_BT$, increasing the chain stiffness will enhance the probability of particles getting adsorbed on the chain more permanently in the time scale of the translocation

process, and hence it will decrease the back-sliding, as is clearly seen in Figs. 4(c) and 4(d). Therefore, the back-sliding of the chain is controlled by the total number of bound BPs and the total force exerted by those BPs. The number of bound BPs and force exerted on the chain by the bound BPs will be discussed in Sec. III D

C. Waiting time distribution and back-sliding

The waiting time distribution $W(s)$ is defined as the amount of time a monomer s spends inside the pore such that

$$\sum_{s=1}^{N}\langle W(s)\rangle = \langle\tau\rangle. \tag{11}$$

Evidently a plot of $W(s) \sim s$ reveals detailed information about the translocation process of the individual monomers. This quantity has been studied in detail in the past for fully flexible chains and more recently for driven translocation of semiflexible chains [22,23], and for translocation driven by binding particles [17]. For the case of driven translocation, the shapes of the plots have been rationalized using TP theory [31]. Here we briefly mention the salient features of $W(s)$ in the presence of binding particles, and we compare the graphs of Fig. 5 with those of Fig. 4.

At low concentration of the BPs, the qualitative features of $W(s) \sim s$ [Figs. 5(a) and 5(b)] and $n_b(s) \sim s$ [Figs. 4(a) and 4(b)] are very similar. However, a point worth noting is that although the back-sliding is reduced drastically for a stiffer chain [Figs. 4(c) and 4(d)], the chain takes a longer time to translocate, as also seen in the $W(s)$ of the individual monomer. This is partly due to the fact that a stiffer chain takes a longer time to translocate, as shown by us previously in the context of driven translocation [22,23], and partly due to the fact that a stiffer translocating segment adsorbs more bound particles (see Fig. 1). For smaller ϵ_c we also notice a slight oscillatory behavior for the middle monomers. Contrary to Figs. 5(a) and 5(b), which look similar to Figs. 4(a) and 4(b), for larger binding strength the behavior of n_b and W is opposite. At a larger binding energy, n_b decreases with the chain stiffness but W increases in general. For low concentrations [Fig. 5(c)],

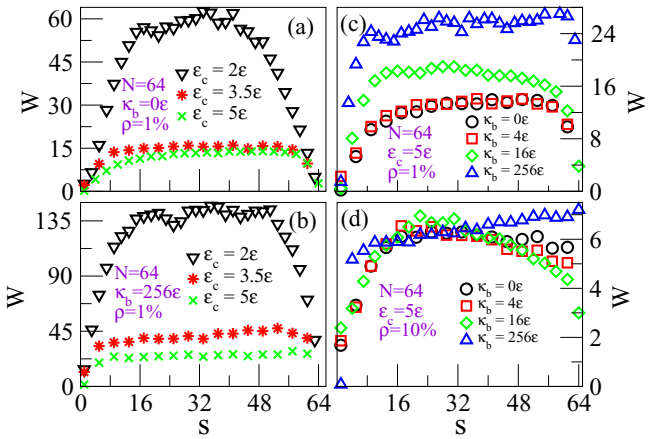

FIG. 5. (Color online) The corresponding waiting time distribution of Fig. 4.

$W(s)$ is distinct for each stiffness. Both Figs. 5(c) and 5(d) share the features of a driven translocation in that the position of the maximum for a stiffer chain shifts toward a smaller value of the monomer index. Also, a noticeable feature is that it is the extreme stiff chain that exhibits very different behavior than the semiflexible chains, whose contour length $L \leqslant \ell_p$. Increasing the concentration of the BPs markedly reduces the values of $W(s)$ and hence the MFPT $\langle\tau\rangle$. The similarity of the variation of the waiting time distribution as a function of chain stiffness for larger strength of the attractive interaction leads us to think that the TP theory can also be extended to the case in which no external bias is present; however, the chemical potential difference may produce an effective force on the chain monomer leading to a propagating tension front.

D. Number of bound BPs and driving force

An important aspect of the polymer translocation facilitated by attractive binding particles is how these particles impart an effective force on the translocating segment and how the force depends on various factors. Since this force is a function of the number of bound particles $n_{\rm bound}(s)$, we first look at this quantity as a function of the translocated segment s as shown in Fig. 6. We also find that the quantity $\tilde{n}_{\rm bound}(s) = n_{\rm bound}(s)/s$ is useful in depicting the evolution of the bound pairs shown in the insets of Figs. 6(a) and 6(b). Several noticeable features of Fig. 6 are the following. We consider two concentrations of the binding particles, namely 1% [Fig. 6(a)] and 10% [Fig. 6(b)] of strength $\epsilon_c = 5\epsilon$. This value of ϵ_c is close to the bending stiffness of the moderately flexible chain ($\kappa_b = 8\epsilon$). We observe that the dependence of $n_{\rm bound}(s)$ on the chain stiffness is markedly different for a stiff chain ($\ell_p \gg L$ or equivalently $\kappa_b \gg \epsilon_c$) than that of a fully flexible chain, or a moderately flexible chain. While for a

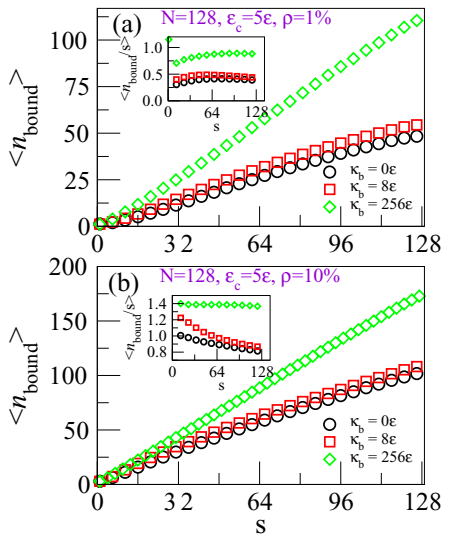

FIG. 6. (Color online) The number of bound BPs on the translocated segment as a function of the s coordinate for (a) 1% and (b) 10% concentration of BPs. The circles (black), squares (red), and diamonds (green) represent fully flexible and semiflexible chains with $\kappa = 0$, 8ϵ, and 256ϵ, respectively. The inset shows the same for the number of bound BPs per unit length.

stiff chain $n_{\rm bound} \propto s$ (or $\tilde{n}_{\rm bound} \approx 0.8$ or 1.4 for 1% and 10% density of the BPs, respectively), $\tilde{n}_{\rm bound}(s)$ either saturates at $\rho = 1\%$ or decreases as a function of s. These qualitative behaviors of $n_{\rm bound}$ as a function of chain stiffness are rightly captured in various snapshots of Fig. 1. As long as $\kappa_b \lessapprox \epsilon_c$, the binding particles are capable of bending the chain, and more than one monomer attach to the same binding particle. For a larger value of $\rho = 10\%$, preexisting bound particles accommodate the incoming translocated monomers and hence $\tilde{n}_{\rm bound}$ decreases. For stiff chains, at least for the concentration considered here, the number of bound particles continues to increase linearly with the translocated segment.

The attractive interaction between the BPs and translocated monomers of the chain cause a net force on the translocated segment of the chain. We calculate the x component (the component in the direction of translocation) of this force as

$$F_x(s) = -\sum_{i=1}^{s}\sum_{j=1}^{N_{\rm BPs}} \frac{\partial U_{\rm binding}(r_{ij})}{\partial x}. \qquad (12)$$

Here, $N_{\rm BPs}$ is the total number of BPs. Figure 7 shows the force F_x due to the BPs along the direction of translocation as a function of $n_{\rm bound}(s)$. For a stiff chain, it is clear that $F_x(s) \propto n_{\rm bound}(s)$, and hence $F_x(s)/n(s)$ remains roughly constant for a stiff chain. For a fully flexible or moderately flexible chain, the force reaches a maximum value that is expected from Fig. 6. For extreme stiff chains, our results are qualitatively

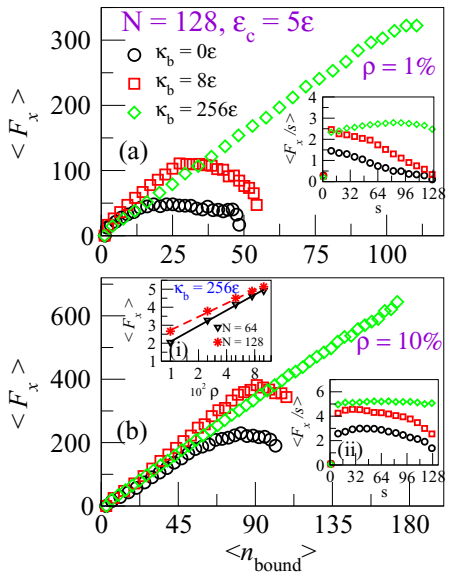

FIG. 7. (Color online) (a) The total force on the translocated segment as a function of the number of bound particles for 1% concentration of BPs. The circles (black), squares (red), and diamonds (green) represent fully flexible and semiflexible chains with $\kappa = 0$, 8ϵ, and 256ϵ, respectively. Inset: the total force on the translocated segment per unit length as a function of the s coordinate. (b) The same as (a) for 10% concentration of BPs. Insets: (i) The asymptotic value of total force on the translocated segment per unit length for a very stiff chain $\kappa_b = 256\epsilon$ as a function of density of the BPs ρ for chain lengths $N = 64$ (red stars) and $N = 128$ (black triangles). The lines are logarithmic fits to the data. (ii) Same as the inset of (a) for a 10% concentration of BPs.

the same as the previous work of Zandi *et al.* [8], who found similar behavior for the translocation of a rod, although they considered the motion of the rod to be restricted along the translocation axis only. In the extreme stiff limit, it is expected that the qualitative feature will be the same. We have also calculated the concentration dependence of the F_x from the asymptotic values of $F_x(s)/n(s)$ in the limit of extreme stiff chains shown in the inset (i) of Fig. 7(b). We find $F_x \propto \ln \rho$ as expected as the free energy is proportional to $\ln \rho$.

E. Universal aspects and scaling of MFPT

We now discuss the MFPT for translocation facilitated by binding particles. The dependence of MFPT on chain length N has been a matter of considerable interest for the past two decades [2], and theoretical studies have achieved a rather mature state in delineating the factors affecting the translocation exponent α ($\langle\tau\rangle \sim N^{\alpha}$).

For the case of driven translocation, a scaling ansatz has been established [24],

$$\langle\tau\rangle = A(f,\eta_{\rm solv})N^{1+\nu} + B(f,\eta_{\rm solv})(\eta_{\rm pore}/\eta_{\rm solv})N. \qquad (13)$$

Here, f, $\eta_{\rm solv}$, and $\eta_{\rm pore}$ are the external force, the solvent friction, and the pore friction, respectively, and A and B are nonuniversal quantities whose numerical values are close to unity. Equation (13) explains the nonuniversal finite-N effect arising out of the second term due to the relative influence of pore friction over solvent friction. Detailed numerical calculations [32] show that the Chuang-Kantor-Kardar limit [33] ($\langle\tau\rangle \sim N^{1+\nu}$) is achieved only in the limit of very large $N \to 10^6$. For a moderate chain length of 100–1000, most of the translocation exponents α reported by various groups is within $2\nu \leqslant \alpha \leqslant 1+\nu$ [34–36]. In the case of translocation assisted by the BPs, we also find that the translocation exponent $\alpha \simeq 1.5$, which is another reason to believe that TP theory can be generalized for chemical-potential-induced tension propagation. In the following subsections, we will discuss how the MFPT depends on the density and strength of the binding particles as well as on the persistence length of the chain.

1. Density dependence of MFPT

Consistent with Eq. (13), we also find that the translocation exponent α is within the above-mentioned bound. This is first verified in Fig. 8, where we observe that the scaled MFPTs $\langle\tau\rangle/N^{1.5}$ for two chain lengths ($N = 64$ and 128) collapse on the same master plot as a function of the density of the BPs. We have already shown that the effective driving force $\langle F_x\rangle$ due to the BPs is a function of chain stiffness κ_b, binding strength ϵ_c, and density ρ of the BPs. It is expected that the MFPT will also satisfy Eq. (13) with an enlarged set of variables, $\langle\tau\rangle \equiv \langle\tau(\tilde{f},\eta_{\rm solv},\eta_{\rm pore},\kappa_b)\rangle$, so that in addition to its dependence on $\eta_{\rm pore}$, $\eta_{\rm solv}$, and κ_b, it will depend on an effective force $\tilde{f} \equiv \tilde{f}(f,\rho,\kappa_b,\epsilon_c)$. which, in addition to f, will now depend on ρ, κ_b, and ϵ_b. The problem considered in this paper is the special case with external bias $f = 0$ and $\langle F_x\rangle \equiv \langle\tilde{f}(\rho,\kappa_b,\epsilon_c)\rangle$. For the low densities considered here, we observe that the MFPT satisfies a power-law dependence on the density of the BPs,

$$\langle\tau\rangle = A\rho^{-\beta}, \qquad (14)$$

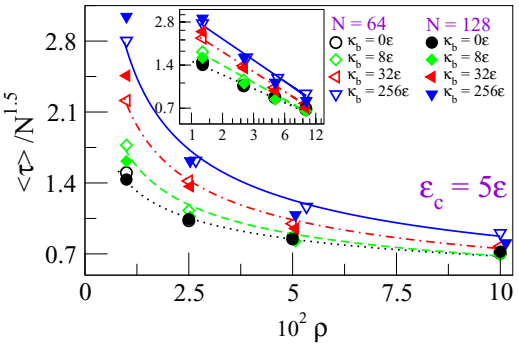

FIG. 8. (Color online) The normalized MFPT as a function of density of the BPs ρ for several values of the stiffness parameter κ_b. The open symbols represent the data for the shorter chain ($N = 64$) and the closed symbols are for the longer chain ($N = 128$). Black circles, green diamonds, red left-triangles, and blue down-triangles represent the chain flexibility $\kappa_b = 0\epsilon$, 8ϵ, 32ϵ, and 256ϵ, respectively. The lines through the points are power-law fits with persistence-length-dependent exponents, and the inset shows the corresponding log-log plot.

where β is a nonuniversal exponent that depends on the persistence length of the chain and the binding strength of the BPs. This aspect can be qualitatively justified by noting that for the low densities, the MFPT will initially decreases significantly as more and more BPs are available to the translocating chain. But the effect will tend to saturate as the number of unbound monomers decreases as the density of the binding particles increases. Thus the dependence is not linear and the dependence of the exponent β on the chain persistence length ℓ_p is expected as the effect of the BPs on a stiffer chain is more pronounced. Evidently, the dependence of MFPT will saturate at moderate densities when the number of binding particles is more than needed. It is also worth noting that one can argue that for a fully flexible chain, the attractive interaction of the BPs with the chain segment can lead to a collapse of the chain,which will speed up the translocation process [37]. However, this argument will not hold for a stiff chain. As a matter of fact, from the figure we observe that for the stiffer chains, the effect of increasing the density of the BPs in reducing the MFPT is more pronounced as compared to a fully flexible chain. Thus an "effective pulling" force is responsible for the reduction of the MFPT.

2. *Binding strength dependence of MFPT*

Now we discuss the effect of the binding strength of the BPs on the MFPT. For a driven translocation process, we know that $\langle\tau\rangle \propto f^{-1}$ [2]. Here, as we just discussed, the dependence of MFPT on the "effective force" $\tilde{f}$ produced by the BPs is expected to be more complex as $\tilde{f} \equiv \tilde{f}(s,\rho,\epsilon_c,\kappa_b)$, in addition to the pore and the solvent friction. We show the dependence of MFPT on ϵ_c in Fig. 9 for a low density of the BPs. We observe that for large binding energies, asymptotes of the rescaled MFPT $\langle\tau\rangle/N^{1.5}$ for different stiffnesses roughly saturate at a common value. From a further analysis of these graphs, we note that for all chain stiffnesses, each curve could be fitted to a polynomial as follows:

$$\langle\tau\rangle/N^{1.5} = a_0 - a_1\epsilon_c + a_2{\epsilon_c}^2 - a_3{\epsilon_c}^3 + a_4{\epsilon_c}^4. \qquad (15)$$

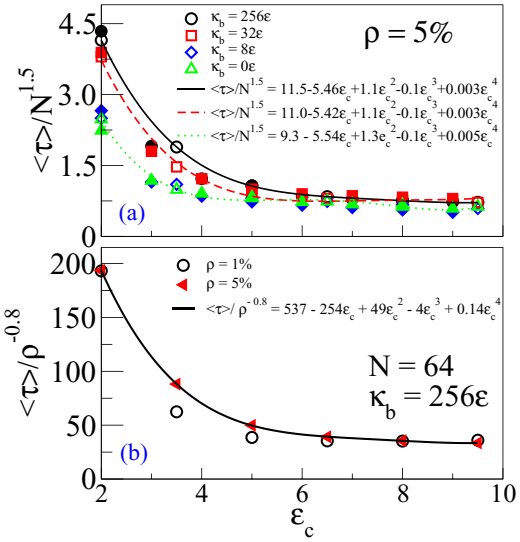

FIG. 9. (Color online) (a) Scaled MFPT $\langle\tau\rangle/N^{1.5}$ as a function of binding strength ϵ_c of BPs for different chain stiffness ($\kappa_b = 0, 8\epsilon$, 32ϵ, and 256ϵ) and for $N = 64$ (open symbols) and $N = 32$ (closed symbols), respectively. Black-solid, red-dashed, and green-dotted lines are fourth-degree polynomial fits to the data for $\kappa_b = 256\epsilon$, 32ϵ, and 8ϵ, respectively. The fitted line for the data corresponding to $\kappa_b = 8\epsilon$ is almost the same as for $\kappa_b = 0\epsilon$. (b) Scaled MFPT $\langle\tau\rangle/\rho^{-0.8}$ as a function of binding strength ϵ_c of BPs for a stiff chain ($\kappa_b = 256\epsilon$) of length $N = 64$. Open symbols correspond to $\rho = 1\%$ and closed symbols correspond to $\rho = 5\%$. The solid line represent the fourth-degree polynomial fit to the data.

We further notice that to a first approximation, $a_1 \simeq 0.5a_0$, $a_2 \simeq 0.1a_0$, $a_3 \simeq 0.01a_0$, and so on. We provide a physical picture as follows, which we have verified for at least two different chain lengths and for several low concentrations of the BPs. The first term a_0 represents the density and stiffness dependence of translocation in the limit $\epsilon_c \to 0$, and approximately we find $a_0 \simeq \rho^{-\beta}$. We have seen before [23] that the MFPT increases with the chain stiffness. Once the attractive BPs are introduced, the translocation acquires the signature of a driven translocation and MFPT decreases, which is reflected in the negative contribution of the linear term $a_1\epsilon_c$. The quadratic term $a_2{\epsilon_c}^2$ and the higher-order terms represent the many-body effect, where two or more binding particles would be attached to the same monomer and introduce "crowding" and increase the MFPT. It is worth noticing that each graph in principle can exhibit minima for a certain combination of coefficients that were reported previously [17,38] but have not been analyzed adequately. We reconfirm our analysis in Fig. 9 by showing the data collapse of $\langle\tau\rangle/\rho^{-0.8}$ for two different concentrations for a stiff chain.

3. *Chain stiffness and MFPT*

Finally in Fig. 10 we analyze the translocation data as a function of the chain stiffness for a moderate strength of the attractive interaction ($\epsilon_c/k_BT \simeq 4\epsilon$) for several densities. For $\ell_p \leqslant L$, the MFPT varies approximately linearly as a function of the chain stiffness. However, beyond $\ell_p \geqslant L$ the strict linearity will no longer be valid as the effect of the chain stiffness will saturate. The inset of Fig. 10 shows the saturation effect.

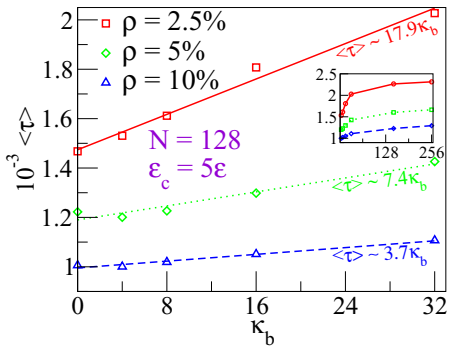

FIG. 10. (Color online) The MFPT varies linearly with the chain rigidity κ_b for smaller values of κ_b. After a certain value of rigidity, the MFPT saturates. Red-squares, green-diamonds, and blue-triangles represent the density $\rho = 2.5\%$, 5%, and 10%, respectively. The inset is the same plotted in log-log scale.

IV. SUMMARY AND DISCUSSION

To summarize, we have studied translocation of a homopolymer through a nanopore in the presence of attractive BPs at the *trans* side responsible for the directed motion of the chain. The motivation of the problem stems from a seminal paper by Simon, Peskin, and Oster [6], which raised an important issue of nonspecific transport in the biological world, which is as generic as diffusion, albeit a faster process, and it suggested directed diffusion rectified by binding particles as a possible solution. As an example, this process occurs in the biological world when DNA enters a nucleopore, and the chaperonin proteins provide the necessary driving force for the translocation. Thus a study of a coarse-grained model is of practical value. Theoretical studies based on idealized and simpler models, based on several assumptions, predict how the attractive BPs enhance the directed diffusion and exert a force on the translocating chain. However, the assumptions are often not satisfied, which was shown in some numerical works in the past. One of the important results is that the ratcheting mechanism introduced through the reversible binding of the BPs under certain conditions can outperform the ideal ratchet. This was demonstrated earlier by Zandi *et al.* [8] for the 1D translocation of a rod. Here we have demonstrated its generic validity.

There is no net external force in this system; however, we have demonstrated that there is an effective pulling force exerted by the attractive BPs on the translocating chain. Indeed, we observe that we can find consistent explanations to some of our simulation data using the original TP theory [31] and the results from our previous simulation studies of driven translocation of a semiflexible chain through a nanopore [23], where we demonstrated how the chain stiffness affects the tension propagation and hence the translocation process. A plausible physical reason for this connection is that unlike the case of driven translocation, here the asymmetry in the chemical potential creates and drives a tension in the *cis* side. Therefore, for the stronger interaction strength of the BPs, the waiting time distribution is asymmetric and qualitatively similar to that of driven translocation. Based on this evidence from simulation results, we have suggested that by generalizing the external force to an effective force so as to include other factors responsible for a pulling force, it is likely that the TP theory can be extended to such a directed diffusion process. In most cases, we have provided scaling relations for the dependence of MFPT on various variables, and phenomenological equations and data collapse in the limit of extreme stiff chains, which will be useful for further theoretical studies.

We would like to comment now on the relevance of our work and the choice of the parameters with regard to actual biological processes. The experimental value of the diffusion coefficient for short chains translocating through a nanopore is $D_{\rm chain} \sim 10^{-8}$ cm^2/s [39,40]. The diffusion constant for the short macromolecules in a cellular solution is $D_{\rm BP} \sim 10^{-6}$ cm^2/s [41], so that the ratio $D_{\rm BP}/D_{\rm chain} \sim 100$. For the parameters used in our simulation, we find that this ratio $D_{\rm BP}/D_{\rm chain} \sim 20 - 50$, which implies that the choice of the parameters can be associated with actual biological processes. We have also checked that the diffusion time of the chain $\tau_{\rm chain} \ll \langle\tau\rangle$. Thus we expect that our numerical studies augmented by good theoretical estimates will promote further theoretical and experimental work in this field.

ACKNOWLEDGMENT

We thank Wokyung Sung and Tapio Ala-Nissila for a careful reading and several critical comments on the manuscript.

[1] B. Alberts *et al.*, *Molecular Biology of the Cell* (Garland, New York, 1994).
[2] For recent reviews in the field, see M. Muthukumar, *Polymer Translocation* (CRC Press, Boca Raton, FL, 2011); A. Milchev, J. Phys.: Condens. Matter **23**, 103101 (2011); D. Panja, J. Stat. Mech. (2010) P06011; V. V. Palyulin, T. Ala-Nissila, and R. Metzler, Soft Matter **10**, 9016 (2014).
[3] A. F. Maltouf and B. Labedan, J. Bacteriol. **153**, 124 (1983).
[4] H. Salman, D. Zbaida, Y. Rabin, D. Chatenay, and M. Elbaum, Proc. Natl. Acad. Sci. USA **98**, 7247 (2001).
[5] K. E. S. Matlack, W. Mothes, and T. A. Rapoport, Cell **92**, 381 (1998); K. E. S. Matlack, B. Misselwitz, K. Plath, and T. A. Rapoport, *ibid.* **97**, 553 (1999).
[6] S. M. Simon, C. S. Peskin, and G. F. Oster, Proc. Natl. Acad. Sci. USA **89**, 3770 (1992).
[7] W. Sung and P. J. Park, Phys. Rev. Lett. **77**, 783 (1996).
[8] R. Zandi, D. Reguera, J. Rudnick, and W. M. Gelbart, Proc. Natl. Acad. Sci. USA **100**, 8649 (2003).
[9] W. Yu, Y. Ma, and K. Luo, J. Chem. Phys. **137**, 244905 (2012).
[10] T. Ambjrnsson and R. Metzler, Phys. Biol. **1**, 77 (2004).
[11] T. Ambjrnsson, M. A. Lomholt, and R. Metzler, J. Phys.: Condens. Matter **17**, S3945 (2005).
[12] R. Metzler and K. Luo, Eur. Phys. J. Spec. Top. **189**, 119 (2010).
[13] R. H. Abdolvahab, F. Roshani, A. Nourmohammad, M. Sahimi, and M. R. R. Tabar, J. Chem. Phys. **129**, 235102 (2008).

[14] R. H. Abdolvahab, M. R. Ejtehadi, and R. Metzler, Phys. Rev. E **83**, 011902 (2011).
[15] R. H. Abdolvahab, R. Metzler, and M. R. Ejtedadi, J. Chem. Phys. **135**, 245102 (2011)
[16] W. Yu and K. Luo, J. Am. Chem. Soc. **133**, 13565 (2011)
[17] W. Yu and K. Luo, Phys. Rev. E **90**, 042708 (2014).
[18] D. Wei, W. Yang, X. Jin, and Q. Liao, J. Chem. Phys. **126**, 204901 (2007).
[19] F. Kapahnke, U. Schmidt, D. W. Heermann, and M. Weiss, J. Chem. Phys. **132**, 164904 (2010).
[20] C. Lorscher, T. Ala-Nissila, and A. Bhattacharya, Phys. Rev. E **83**, 011914 (2011).
[21] *Feynman Lectures*, edited by R. P. Feynman, R. B. Leighton, and M. Sands (Addison-Wesley, Reading, MA, 1963), Vol. II.
[22] A. Bhattacharya, Polymer Sci. Ser. C **55**, 60 (2013).
[23] R. Adhikari and A. Bhattacharya, J. Chem. Phys. **138**, 204909 (2013).
[24] T. Ikonen, A. Bhattacharya, T. Ala-Nissila, and W. Sung, Europhys. Lett. **103**, 38001 (2013).
[25] G. S. Grest and K. Kremer, Phys. Rev. A **33**, 3628 (1986).
[26] W. F. van Gunsteren and H. J. C. Berendsen, Mol. Phys. **45**, 637 (1982).
[27] P. G. de Gennes, *Scaling Concepts in Polymer Physics* (Cornell University Press, Ithaca, NY, 1979).
[28] M. Rubinstein and R. H. Colby, *Polymer Physics* (Oxford University Press, Oxford, 2003).
[29] A. Huang, A. Bhattacharya, and K. Binder, J. Chem. Phys. **140**, 214902 (2014).
[30] For stiff chains, the total force on the chain increases linearly with the number of bound particles n_b, which is proportional to the physical dimension d (Fig. 7). We also know that $\langle\tau\rangle \propto 1/F$ [2], which implies that $\langle\tau\rangle \propto 1/d$. Thus from Eq. (10), to a first approximation $\tau_{\rm ratchet}/\langle\tau\rangle$ will be independent of the physical dimension d. However, how the "perfect ratchet" condition will be over- or undersatisfied will depend on the parameters of the model.
[31] T. Sakaue, Phys. Rev. E **76**, 021803 (2007); **81**, 041808 (2010).
[32] T. Ikonen, A. Bhattacharya, T. Ala-Nissila, and W. Sung, J. Chem. Phys. **137**, 085101 (2012)
[33] J. Chuang, Y. Kantor, and M. Kardar, Phys. Rev. E **65**, 011802 (2001).
[34] Simulation of short chains by various groups produced a translocation exponent $\alpha \simeq 1.5$ [35,36]. Realizing that in two dimensions $2\nu = 1.5$, an explanation has been given that for short chains, $\langle\tau\rangle \sim N^{2\nu}$ [35]. According to more recent theories [24,32], it is perceived as a finite chain length effect.
[35] K. Luo, I. Huopaniemei, T. Ala-Nissila, and S-C. Ying, J. Chem. Phys. **124**, 114704 (2006).
[36] A. Bhattacharya, in *Computer Simulation Studies in Condensed Matter Physics XXII*, edited by D. P. Landau, S. P. Lewis, and H. B. Schuttler, Physics Proceedia Vol. 3 (Elsevier, Amsterdam, 2010), p. 1411.
[37] K. Sneppen and G. Zocchi, *Physics in Molecular Biology* (Cambridge University Press, Cambridge, 2005).
[38] A. Bhattacharya, T. Ala-Nissila, and W. Sung, Bull. Am. Phys. Soc., APS March Meeting 2011 (APS, New York, 2011), Vol. 56, Abstract Q43.00012.
[39] J. F. Chauwin, G. Oster, and B. S. Glick, Biophys. J. **74**, 1732 (1998).
[40] C. S. Peskin, G. M. Odell, and G. F. Oster, Biophys. J. **65**, 316 (1993).
[41] A. S. Verkman, Trends Biochem. Sci. **27**, 27 (2002).